

Evaluating GPT-V4 (GPT-4 with Vision) on Detection of Radiological Findings on Chest Radiographs

Yiliang Zhou, MS¹, Hanley Ong, MD², Patrick Kennedy, MD², Carol Wu, MD³, Jacob Kazam, MD², Keith Hentel, MD, MS², Adam Flanders, MD⁴, George Shih, MD^{*2}, and Yifan Peng, PhD^{1,*}

¹Department of Population Health Sciences, Weill Cornell Medicine, New York, NY 10065

²Department of Radiology, Weill Cornell Medicine, New York, NY 10065

³Department of Thoracic Image, University of Texas MD Anderson Cancer Center, Houston, TX 77030

⁴Department of Radiology, Thomas Jefferson University Hospital, Philadelphia, PA 19107

*Corresponding: ges9006@med.cornell.edu, yip4002@med.cornell.edu

Abstract

Background

Generating radiological findings from chest radiographs is pivotal in medical image analysis. The emergence of GPT-4 with vision (GPT-4V) has opened new perspectives on the potential for automated image-text pair generation. However, the application of GPT-4V to real-world chest radiography is yet to be thoroughly examined.

Purpose

To investigate GPT-4V's capability to generate radiological findings from real-world chest radiographs.

Materials and Methods

In this retrospective study, 100 chest radiographs with free-text radiology reports were annotated by a cohort of two radiology-attending physicians and three residents to establish a reference standard. Out of 100 chest radiographs, 50 were randomly picked from the National Institutes of Health (NIH) chest radiography data set, and 50 were randomly selected from the Medical Imaging and Data Resource Center (MIDRC). The performance of GPT-4V at detecting imaging findings from each chest radiograph was assessed in the zero-shot settings (where it operates without prior examples) and few-shot settings (where it operates with two examples). Its outcomes were compared with the reference standard about radiological conditions, their corresponding codes in the International Classification of Diseases, Tenth Revision (ICD-10 codes), and laterality.

Results

In the zero-shot setting, in the task of detecting ICD-10 codes alone, GPT-4V attained an average PPV of 12.3%, an average TPR of 5.8%, and an average F1 score of 7.3% on the NIH dataset, and an average PPV of 25.0%, an average TPR of 16.8%, and an average F1 score of 18.2% on the MIDRC dataset. When both the ICD-10 codes and their corresponding laterality were considered, GPT-4V produced an average PPV of 7.8%, an average TPR of 3.5%, and an average F1 score of 4.5% on the NIH dataset, and an average PPV of 3.6%, an average

TPR of 4.9%, and an average F1 of 6.4% on the MIDRC dataset. In few-shot learning, GPT-4V showed improved performance on both datasets. When contrasting zero-shot and few-shot learning, there were improved average TPR and F1 scores in few-shot learning. Nonetheless, there was not a substantial increase in the average PPV.

Conclusion

Although GPT-4V showed promise in understanding real-world images but had limited effectiveness in interpreting real-world chest radiographs.

1 Introduction

Generating radiological findings from chest radiographs is pivotal in medical image analysis[1]. Recent advancements in fine-tuned pretrained models have showcased their capability to translate image content into text[2]. However, these models are often trained on extensive, non-specific datasets and may need more domain-specific tuning for chest radiographs. The emergence of OpenAI’s GPT-4 with vision (GPT-4V), a multimodal large language model (LLM) with visual recognition, has opened new perspectives on the potential for automated image-text pair generation in the medical care domain. Advanced multimodal LLMs, such as GPT-4V, can understand both text and images. While several studies have investigated the performance of GPT-4 in generating radiological impressions[3] and summarizing clinical trials[4], the practical application of multimodal LLMs to real-world chest radiographs is yet to be thoroughly examined. Motivated by this gap, this study aimed to investigate GPT-4V’s capability to generate radiological findings from real-world chest radiographs.

2 Materials & Methods

Because of the publicly available nature of the data set used in this study, the requirement to obtain written informed consent from all subjects was waived by the institutional review board.

2.1 Study Design and Data Collection

In this retrospective study, a total of 100 chest radiographs and reports were independently annotated by a cohort of two radiology-attending physicians and three residents to establish a reference standard (Figure 1). Out of 100 chest radiographs, 50 chest radiographs were randomly picked from the National Institutes of Health (NIH) chest radiography data set, and their corresponding reports were dictated by one radiology-attending physician and three radiology residents[3]. These 50 patients have been previously reported[4]. The prior article dealt with the generation of the impression section using the finding section in the reports, whereas this article reports on the generation of a radiological finding table from the images.

The remaining 50 chest radiographs and de-identified free-text radiology reports were randomly selected from the Medical Imaging and Data Resource Center (MIDRC)[4]. Each report included a Findings section and an Impressions section.

Out of 100 chest radiographs and reports, 10 cases were randomly selected (5 from the NIH dataset and 5 from the MIDRC dataset), and two were randomly selected to serve as few-shot examples for the GPT-4V model. The remaining 90 were used to evaluate GPT-4V’s performance in zero-shot learning scenarios, where it operates without prior examples, and in few-shot learning scenarios, where it operates with two examples. Its outcomes were then compared with the reference standard annotated by radiologists about clinical conditions, their corresponding codes in the International Classification of Diseases, Tenth Revision (ICD-10), and laterality.

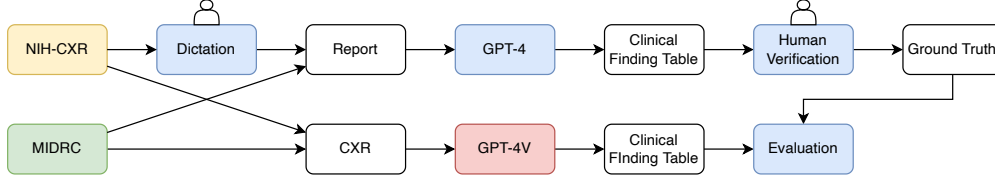


Figure 1: The workflow of data construction and model application. GPT-4V=GPT-4 with vision, MIDRC= Medical Imaging and Data Resource Center, NIH= National Institutes of Health

2.2 GPT-4 with Vision (GPT-4V)

GPT-4V (Oct.13th, 2023 version; OpenAI) was used. This version of GPT enables users to instruct GPT-4 to analyze image inputs.

2.3 Experimental setup

To obtain the reference standard tables, GPT-4 was used to convert each free-text radiology report (Figure 2a) into a table of radiological findings with the prompt shown in Figure 2b. This table included the radiological findings, the corresponding ICD-10 diagnostic codes and their laterality, and detailed descriptions of the ICD codes (Figure 2c). Subsequently, each report was independently evaluated by three readers from a cohort of five board-certified radiologists and residents (H.O., P.K., C.W., J.K., G.S). Two of the readers were third-year radiology residents, and the remaining three are radiology attendings, each with over 15 years of experience. Their radiology subspecialties cover chest, ED/bone, neurology, and body imaging. All readers had access to the image views and reports but not to additional clinical or patient data. Both datasets, the National Institutes of Health (NIH) and the Medical Imaging and Data Resource Center (MIDRC), were comprehensively reviewed, with each dataset’s 50 reports being examined by three reviewers to maintain consistency and objectivity in the evaluation process. Findings were only included in the final tables if they were observed by at least two of the three reviewers; conversely, findings were excluded if two or more reviewers did not identify them. The majority vote principle was employed to provide a clear consensus for the presence or absence of radiological findings and lead to the final reference-standard table.

2.3.1 Evaluating Performance in the zero-shot setting

To evaluate GPT-4V’s performance in the zero-shot setting, the chest radiographs (Figure 2d) were input into the GPT-4V model (version from Oct.13th)[2] along with the prompt (Figure 2e). This step aims to generate a radiological findings table (Figure 2f) comparable to the reference standard. The analysis concentrated on aligning positive radiological finding identification and laterality between GPT-generated and consensus tables. Positive predictive value (PPV), true positive rate (TPR), and F1 scores were calculated at the report level (detailed in the section of “Evaluation metrics”). Notably, the application of the F1 scores represented an unconventional approach due to the potential involvement of multiple diagnoses. These metrics were used to assess the accuracy of GPT-4V in detecting the ICD-10 codes and their respective laterality.

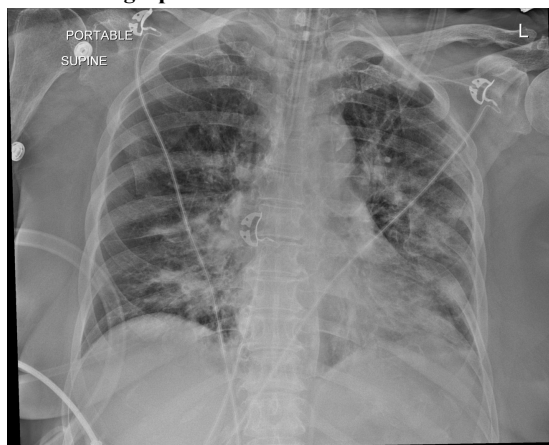
2.3.2 Evaluating Performance in the few-shot setting

To evaluate GPT-4V’s performance in the few-shot setting, the input was extended to include two examples of chest radiographs with their corresponding radiological findings tables before the prompt. From the pool of 10 chest radiographs, two were randomly selected to serve as few-shot examples for the GPT-4V model. Supplying the model with these examples helped to provide context, boosting the model’s capacity to generate an accurate radiological findings table. The same performance metrics— PPV, TPR, and F1 score— were used at the report level to assess the effectiveness of few-shot learning.

a. Radiology report

Procedure: Single AP view of the chest
History: cough
Comparison: None
Findings: Tip of the endotracheal tube is 2 cm from the carina. The cardiomeastinal silhouette is within normal limits. Bilateral pulmonary opacities are noted. A small left pleural effusion is present.
Impression: Bilateral pulmonary opacity suspicious for pneumonia

d. Chest radiograph



b. Prompt to convert the free-text report into a table of radiological findings

Read the report and look for any important clinical findings. Provide a summary in a table format where the positive clinical conditions are 1 and the negative clinical conditions are 0. Designate each condition as left side, right side, or bilateral. Provide an ICD-10 code in a separate column for positive findings only or N/A if not applicable.

Table columns include: [Exam No., Finding No., Clinical Finding, Left Side, Right Side, Bilateral, Midline, ICD-10 Code, ICD-10 Description]

Additional instructions:

1. Normal findings should be excluded from each table
2. Group similar findings together where possible for each table
3. Create a table

e. Prompt to read a chest radiograph and generate a table of radiological findings

Examine this image and look for any important clinical findings. Provide a summary in a table format where the positive clinical conditions are 1 and the negative clinical conditions are 0. Designate each condition as left side, right side, or bilateral. Provide an ICD-10 code in a separate column for positive findings only or N/A if not applicable.

Table columns include: [Exam No., Finding No., Clinical Finding, Left Side, Right Side, Bilateral, Midline, ICD-10 Code, ICD-10 Description]

Additional instructions:

1. Normal findings should be excluded from each table
2. Group similar findings together where possible for each table
3. Create a table

c. The table of reference standard radiological findings

Radiological Finding	Location	ICD-10	ICD-10 Description
Pulmonary Infiltrate	Right Side	R91.8	Other nonspecific abnormal finding of lung field
Pleural Effusion	Right Side	J90	Pleural effusion, not elsewhere classified
Consolidation	Right Side	J18.9	Pneumonia, unspecified organism
Cardiomegaly	Midline	I51.7	Cardiomegaly
Medical Devices Present	Bilateral	Z96.0	Presence of urogenital implants

f. GPT-4v-generated results

Radiological Finding	Location	ICD-10	ICD-10 Description
Endotracheal tube placement	Midline	Z93.0	Tracheostomy status
Pulmonary opacities	Bilateral	J84.9	Interstitial pulmonary disease, unspecified
Pleural effusion	Left Side	J90	Pleural effusion, not elsewhere classified
Pneumonia	Bilateral	J18.9	Pneumonia, unspecified organism

Figure 2: An example. a, The radiology report. b, The prompt used to convert the free-text report into a table of radiological findings. c, The table of radiological findings that has been confirmed by radiologists using the report. d, The chest radiography input of GPT-V. e, The prompt utilized by GPT-4V to create a table of radiological findings derived from the chest radiography. f, The result produced by GPT-4V.

2.4 Statistical Analysis

When obtaining the final reference standard tables, the interrater agreement was reported using Cohen’s Kappa score[5].

First, the GPT-4V was employed to detect radiological findings from each chest radiography and compared the predicted findings with those obtained from the radiologists. To convey the performance evaluation, positive predictive value (PPV) was utilized to denote the proportion of ICD-10 Codes correctly predicted by GPT-4V, while the true positive rate (TPR) represented the ration of true positive predictions to the total number of ICD-10 Codes identified by GPT-4V.

Evaluation metrics of PPV, TPR, and F1 score were used to assess GPT-4V’s performance in detecting imaging findings from each chest radiograph [6]. These predicted findings were then compared with those obtained from the radiologists.

$$F1 = 2 * \frac{PPV * TPR}{PPV + TPR}$$

In the evaluation of detecting ICD-10 codes, a radiological finding was considered a true positive if its ICD-10 code aligned with that in the reference standard table. In evaluating both the radiological findings in ICD codes and their corresponding lateralities, a radiological finding was considered a true positive if both its ICD-10 code and laterality matched those in the reference standard table.

For example, in Figure 2, while evaluating ICD-10 codes alone, there were 2 ICD-10 Codes correctly predicted by GPT-4V (J90 and J18.9), five findings predicted by GPT-4V, and four in the reference standard table. Therefore, PPV was 0.4 ($=2/(2+3)$), TPR was 0.5 ($=2/(2+2)$), and F1 score was 0.44.

After obtaining the PPV, TPR, and F1 score for each chest radiography, the macro averages were calculated for PPV, TPR, and F1 score across all 90 chest radiographs.

In this study, the statistical significance was set at 0.05, and two-tailed t-tests were used for calculating the *P* values for the performance metrics of GPT-4V in detecting radiological findings from chest radiography, specifically assessing the detection of findings represented by ICD codes and their associated lateralities in both zero-shot and few-shot settings.

3 Results

3.1 Performance in the zero-shot setting

The performance of the GPT-4V model in the zero-shot setting varied across the NIH and MIDRC datasets and under different circumstances (Figure 3). In the task of detecting ICD-10 codes alone, the model attained an average PPV of 5.53/45 (12.3%), with a standard deviation (SD) of 0.25, a standard error (SE) of 0.04, and an interquartile range (IQR) of 0.20; an average TPR of 2.60/45 (5.8%), with a SD of 0.10, a SE of 0.02, and an IQR of 0.10; and an average F1 score of 3.30/45 (7.3%), with a SD of 0.13, a SE of 0.02, and an IQR of 0.14, on the NIH dataset. Conversely, on the MIDRC dataset, the model managed an average PPV of 11.25/45 (25.0%), with a SD of 0.24, a SE of 0.04, and an IQR of 0.33; an average TPR of 7.56/45 (16.8%), with a SD of 0.20, a SE of 0.03, and an IQR of 0.25; and an average F1 score of 8.20/45 (18.2%), with a SD of 0.17, a SE of 0.03, and an IQR of 0.29. The notable differences in measurements between the two datasets were primarily due to the MIDRC dataset having fewer missing GPT-4V-generated ICD-10 codes than the NIH dataset. On the MIDRC dataset, GPT-4V generated 144 radiological findings, while the reference standard comprised 261 findings. However, on the NIH dataset, GPT-4V produced 102 radiological findings, while the reference standard comprised 220 findings. Nevertheless, when both the ICD-10 codes and their corresponding laterality were taken into account, the GPT-4V model in the zero-

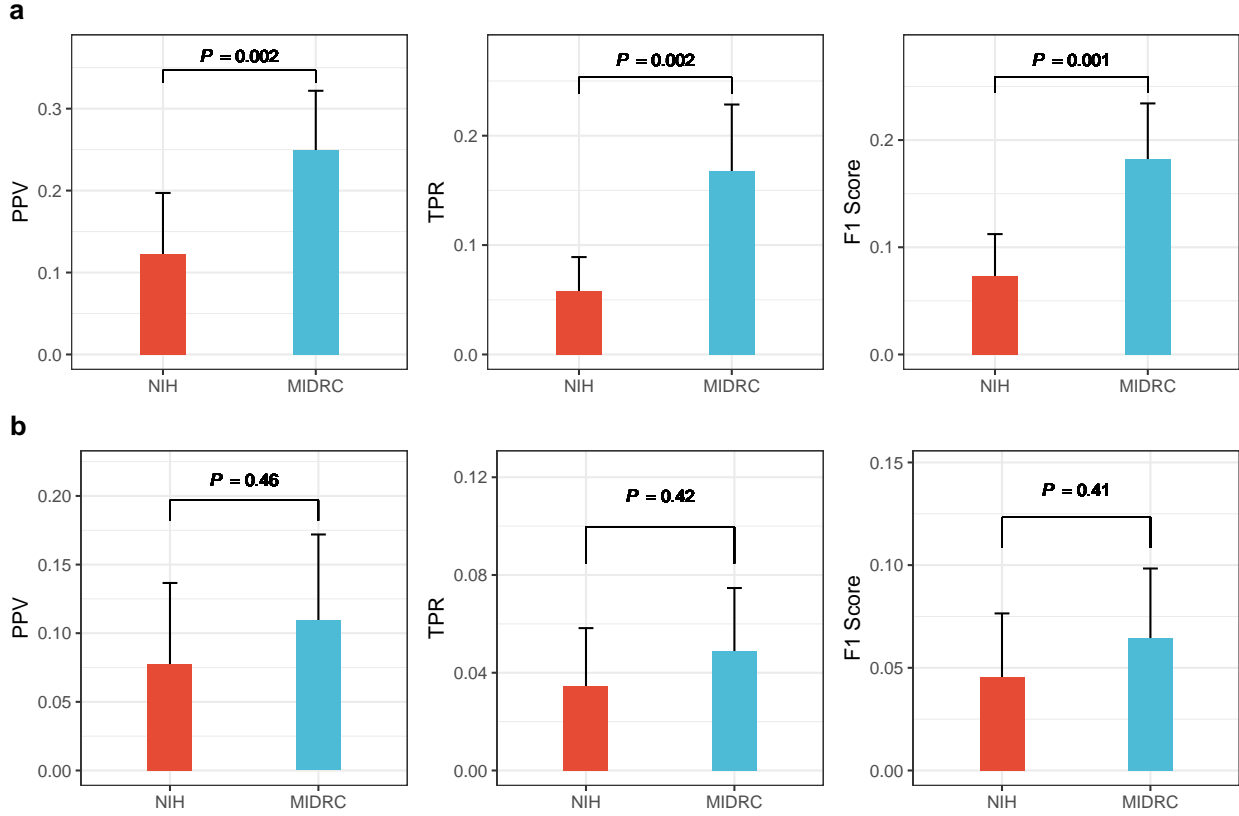


Figure 3: Performance of GPT-4 with Vision (GPT-4V) in the detection of radiological findings from chest radiography in the zero-shot setting, with statistical significance assessed using a two-tailed t-test. a, Detecting the radiological findings in ICD codes. b, Detecting both the radiological findings in ICD codes and their corresponding lateralities. ICD= International Classification of Diseases, Tenth Revision.

shot setting produced an average PPV of 3.5/45 (7.8%), with a SD of 0.20, a SE of 0.03, and an IQR of 0.0; an average TPR of 1.56/45 (3.5%), with a SD of 0.01, a SE of 0.01, and an IQR of 0.0; and an average F1 score of 2.05/45 (4.5%) with a SD of 0.10, a SE of 0.02, and an IQR of 0.0 on the NIH dataset; and an average PPV of 4.92/45 (3.6%), with a SD of 0.21, a SE of 0.03, and an IQR of 0.25; an average TPR of 2.19/45 (4.9%), with a SD of 0.09, a SE of 0.01, and an IQR of 0.10; and an average F1 of 2.90/45 (6.4%), with a SD of 0.11, a SE of 0.02, and an IQR of 0.15, on the MIDRC dataset.

3.2 Performance in the few-shot setting

In few-shot learning, GPT-4V showed improved performance on both NIH and MIDRC datasets (Figure 4). When the model was provided with two illustrative chest radiographs and reports, there was a marked improvement in the average PPV on the NIH dataset, with rates rising to 5.72/45 (12.7%) with a SD of 0.19, a SE of 0.03, and an IQR of 0.25. Average TPR also enhanced to 4.69/45 (10.4%), with a SD of 0.17, a SE of 0.03, and an IQR of 0.22; and the average F1 score reached 5.03/45 (11.1%), with a SD of 0.17, a SE of 0.03, and an IQR of 0.22. On the MIDRC dataset, the average PPV was improved to 16.15/45 (35.9%), with a SD of 0.23, a SE of 0.03, and an IQR of 0.50; the average TPR improved to 16.68/45 (37.1%), with a SD of 0.23, a SE of 0.03, and an IQR of 0.50; and the average F1 score improved to 15.47/45 (34.3%), with a SD of 0.23, a SE of 0.03, and an IQR of 0.50. When tasked with detecting both ICD-10 codes and their corresponding lateralities, the GPT-4V model demonstrated improved efficacy. On the NIH dataset, it displayed an average PPV of 1.62/45(3.5%), with a SD of 0.10, a SE of 0.01, and an IQR of 0.0; an average

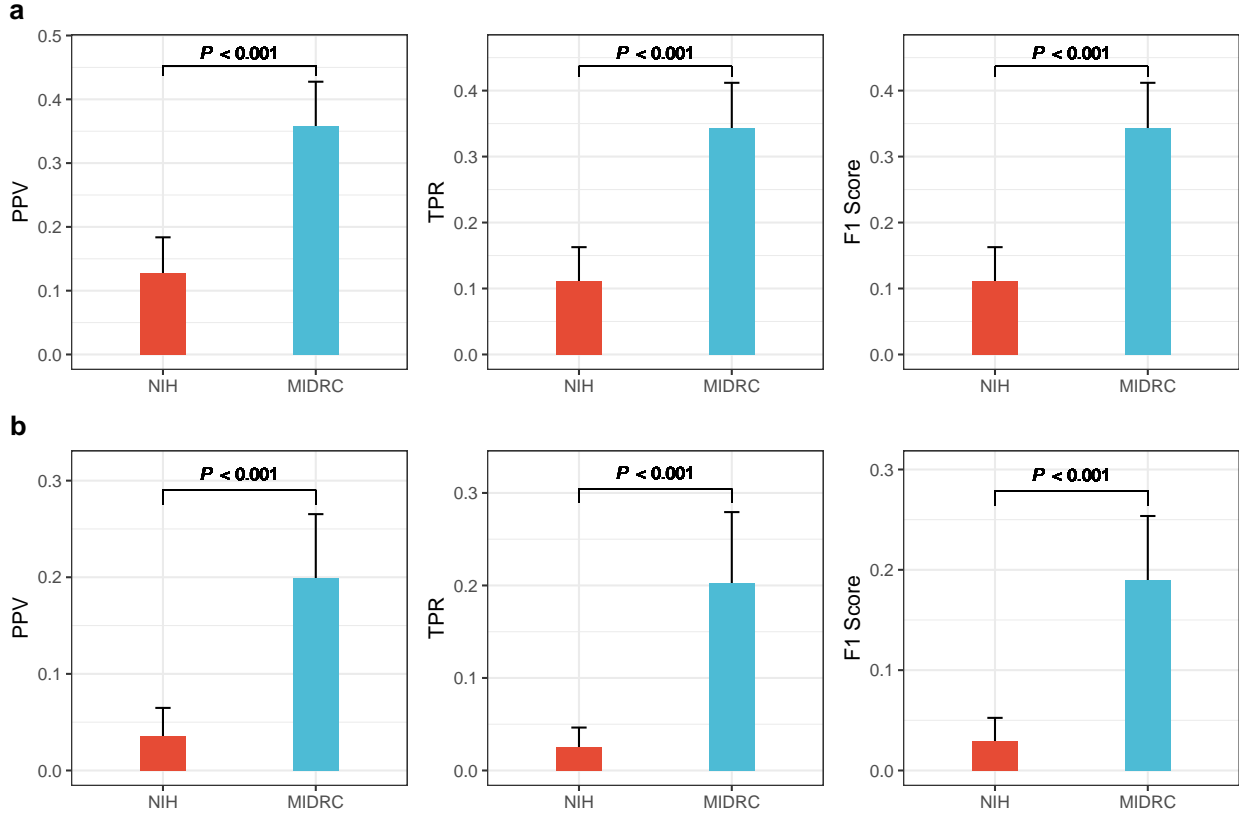


Figure 4: Performance of GPT-4 with Vision (GPT-4V) in the detection of radiological findings from chest radiography in the few-shot setting, with statistical significance assessed using two-tailed t-test. a, Detecting the radiological findings in ICD codes. b, Detecting both the radiological findings in ICD codes and their corresponding lateralities. ICD= International Classification of Diseases, Tenth Revision.

TPR of 1.14/45 (2.5%), with a SD of 0.07, a SE of 0.01, and an IQR of 0.0; and an average F1 score of 1.30/45(2.8%), with a SD of 0.08, a SE of 0.01, and an IQR of 0.0. On the MIDRC dataset, it achieved an average PPV of 8.96/45 (19.9%), with a SD of 0.22, a SE of 0.03, and an IQR of 0.33; an average TPR of 9.14/45 (20.3%), with a SD of 0.25, a SE of 0.04, and an IQR of 0.33; and an average F1 score of 8.53/45 (19.0%), with a SD of 0.21, a SE of 0.03, and an IQR of 0.31.

When contrasting zero-shot and few-shot learning approaches on both datasets (Figure 5), there were improved average TPR and F1 scores in few-shot learning in both scenarios (ICD-10 codes only and ICD-10 codes with laterality). Nonetheless, there was not a substantial increase in the average PPV suggesting that while few-shot learning may enhance the model's capacity to detect findings, it does not noticeably enhance the precision of the predictions.

3.3 Inter-rater Agreement

The study compared each reader's outcomes to the reference standard to evaluate their interpretations (Table 1). On the NIH dataset, the IRA for Reviewer A was 0.78, for Reviewer C was -0.06, and for Reviewer D was 0.96. On the MIDRC dataset, the IRA for Reviewer B was 0.96, for Reviewer C was 0.82, and for Reviewer D was 0.99.

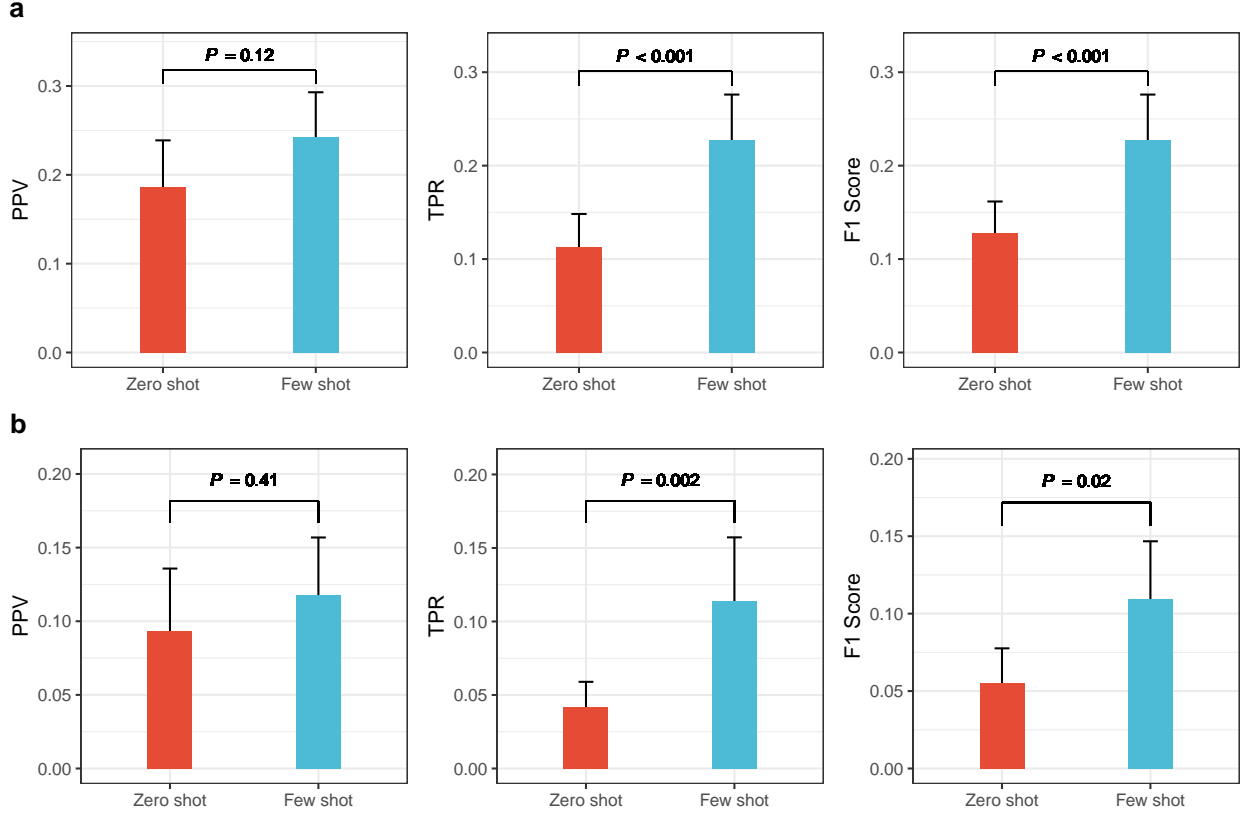


Figure 5: Difference of performance of GPT-4 with Vision (GPT-V4) in the detection of radiological findings from chest radiography between zero-shot and few-shot settings, with statistical significance assessed using two-tailed t-test. a, Detecting the radiological findings in ICD codes. b, Detecting both the radiological findings in ICD codes and their corresponding lateralities.

Table 1: Reviewer Agreement (Cohen’s Kappa) for NIH and MIDRC. The Inter-rater Agreement (IRA) between each reviewer and the reference standard table for both NIH and MIDRC datasets. $k = 1$ indicates perfect agreement among reviewers and the reference standard; $k = 0$ indicates that agreement is no better than chance; $k = -1$ indicates perfect disagreement.

	NIH Results	MIDRC Results
Reviewer A	0.78	NA
Reviewer B	NA	0.96
Reviewer C	-0.06	0.82
Reviewer D	0.96	0.99

4 Discussion

The emergence of multimodal large language models (LLMs) that can understand both text and images, such as GPT-4 with Vision (GPT-4V), shows potential for automated image-text pair generation. However, applying these models to real-world data is yet to be thoroughly examined. This study assessed the feasibility of using GPT-4V to detect radiological findings from chest radiographs in both zero-shot and few-shot learning contexts. The results (average PPV of 5.53/45 (12.3%) and average TPR of 2.60/45 (5.8%)) demonstrated that radiological findings tables generated by the GPT-4V model still need to be prepared for use in clinical practice. We acknowledged a limitation in employing GPT-4 for converting radiological reports into a structured table, where inaccuracies in ICD-10 code assignments and distinguishing between radiological findings and conclusions may impact the data’s reliability and interpretability. A notable limitation of the GPT-4V output was its failure to detect several radiological conditions based on corresponding codes in the International Classification of Diseases, Tenth Revision (ICD-10). Overall, the top three findings that GPT-4V could not detect were “endotracheal tube”, “central venous catheter”, and “degenerative changes of osseous structures”. Conversely, GPT-4V most accurately detected findings such as “chest drain”, “air-space disease”, and “lung opacity”.

Although GPT-4V showed promise in understanding real-world images[7], its effectiveness in interpreting real-world chest radiographs was limited.

Our study had limitations. First, the few-shot training is that it may be more prone to generating ICD-10 codes already in the provided examples, potentially reducing the diversity of ICD-10 codes generated. Second, we were unable to access other multimodal LLMs that support image inputs. Consequently, we lacked comparative data with respect to the results of GPT-4v. Finally, due to the limited size of the dataset and relatively low level of inter-rater agreement among the radiologists, analysis by GPT-4V may have been challenging.

In conclusion, GPT-4 with Vision (GPT-4V) showed promise in understanding natural images but had limited effectiveness in interpreting real-world chest radiographs. Our results highlight the need for additional comprehensive development and assessments prior to incorporating the GPT-4V model into clinical practice routines. Task-specific, fine-tuned multimodal LLMs or foundation models are urgently needed for this purpose, although it is not necessarily the best solution. To yield robust and generalizable results, we plan to explore larger and more diverse datasets using real-world data in future studies. This will involve including multiple modalities, such as brain CT scans and MRIs, to conduct a more thorough evaluation of GPT-4V’s performance.

Acknowledgment

This work was supported by the National Institutes of Health under Award No. 4R00LM013001 (Peng), NSF CAREER Award No. 2145640 (Peng), and Amazon Research Award (Peng, Shih).

We acknowledge parts of this article were generated with GPT-4V (powered by OpenAI’s language model; <https://openai.com>).

References

- [1] Speets AM, van der Graaf Y, Hoes AW, Kalmijn S, Sachs AP, Rutten MJ, Gratama JWC, Montauban van Swijndregt AD, Mali WP. Chest radiography in general practice: indications, diagnostic yield and consequences for patient management. *Br J Gen Pract.* 2006 Aug;56(529):574–578. PMID: 16882374. PMCID: PMC1874520.
- [2] Yang Z, Li L, Lin K, Wang J, Lin CC, Liu Z, Wang L. The Dawn of LMMs: Preliminary Explorations with GPT-4V(ision). *ArXiv.* 2023 Sep;abs/2309.17421. doi: 10.48550/arXiv.2309.17421.

- [3] Wang X, Peng Y, Lu L, Lu Z, Bagheri M, Summers RM. ChestX-Ray8: Hospital-Scale Chest X-Ray Database and Benchmarks on Weakly-Supervised Classification and Localization of Common Thorax Diseases. In: 2017 IEEE Conference on Computer Vision and Pattern Recognition (CVPR); 2017. p. 3462–3471. doi: 10.1109/CVPR.2017.369.
- [4] Sun Z, Ong H, Kennedy P, Tang L, Chen S, Elias J, Lucas E, Shih G, Peng Y. Evaluating GPT4 on Impressions Generation in Radiology Reports. *Radiology*. 2023 Jun;307(5):e231259. doi: 10.1148/radiol.231259. PMID: 37367439.
- [5] Waisberg E, Ong J, Masalkhi M, Kamran SA, Zaman N, Sarker P, Lee AG, Tavakkoli A. GPT-4: a new era of artificial intelligence in medicine. *Ir J Med Sci*. 2023 Dec;192(6):3197–3200. doi: 10.1007/s11845-023-03377-8. PMID: 37076707.
- [6] Seabold S, Perktold J. Statsmodels: Econometric and statistical modeling with Python. *PROC OF THE 9th PYTHON IN SCIENCE CONF (SCIPY 2010)*. 2010:92–96. doi: 10.25080/MAJORA-92BF1922-011.
- [7] Zhang X, Lu Y, Wang W, Yan A, Yan J, Qin L, Wang H, Yan X, Wang WY, Petzold LR. GPT-4V(ision) as a Generalist Evaluator for Vision-Language Tasks. *ArXiv*. 2023 Nov.